COMPARISON BETWEEN TWO CYCLOSTATIONARY DETECTORS FOR RFI MITIGATION IN RADIO ASTRONOMY

Stéphanie Bretteil and Rodolphe Weber

LESI – Polytech'Orléans
Université d'Orléans BP 6744, 45067 Orléans cedex 2, France
phone: +33 2 38494537, fax: +33 2 38417245, email: stephanie.bretteil@univ-orleans.fr
web: www.obs-nancay.fr/rfi

ABSTRACT

Radio astronomers have to observe some celestial emissions at frequencies allocated to an increasing number of active users of the spectrum. This paper presents a scheme for removing efficiently cyclostationary radio frequency interferences (RFI) from astronomical data. Two cyclostationary detectors are compared and computer simulations are used to describe the applicability of these methods.

1. INTRODUCTION

Radio astronomy studies the emissions of celestial sources through the radio spectrum. However, the exponential expansion of the telecommunications makes these emissions more and more corrupted by man-made radio emissions (see Fig. 1). Therefore, RFI mitigation is becoming a necessity in radio astronomy.

Various methods have been experimented to eliminate those RFI depending on the type of interferences and the type of instruments [1]. The present study focuses on time-frequency blanking on data coming from a single dish. Time-frequency blanking consists in removing polluted data blocks in the time-frequency plane before integration in order to clean up the spectrum. The time-frequency plane is obtained in real time by a digital filter bank based on FFT or polyphase filter [2]. The blanking decision depends on the kind of detectors implemented.

The detection criteria are generally based on a statistical contrast between the signal of interest (SOI) and the RFI. For example, the most used criterion is the power estimation. Indeed, its low complexity makes it possible real time implementation. But, its effectiveness depends on the RFI level which must be obviously high. Moreover, the probability of false alarm may increase rapidly if the reference level is not stationary or if the SOI becomes so bright that the system may blank both the RFI and the SOI.

This paper presents two detectors based on the temporal properties of a particular class of RFI, called the cyclostationary signals. These detectors are power independent. Besides they can work with real time constraints and detect RFI with a low Interference Signal Ratio (ISR).

The first section will present the hypothesis and the properties of the signals used in this paper. The second one will define the cyclostationarity and will compare the two detectors. In the third section, an example of time-frequency blanking is described and discussed.

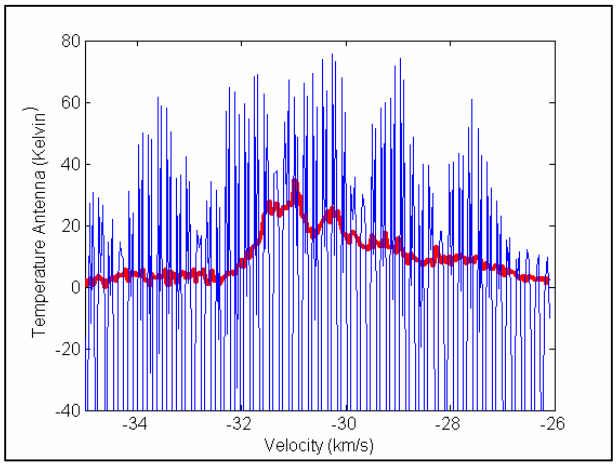

Figure 1: Example of a polluted radio astronomical spectrum (velocity is proportional to frequency). The red smoothed line corresponds to the expected profile of the celestial source (circumstellar envelope of the late-type star OH 104.9). The blue spikes are due to a satellite emission.

2. THE OBSERVATIONAL HYPOTHESES

The purpose of this study is to detect the presence of a cyclostationary RFI in the received signal s(t). The problem can be seen as a classical hypotheses test:

$$\begin{cases} H_0 : s(t) = u(t) \\ H_1 : s(t) = u(t) + b(t) \end{cases} \quad (1)$$

where u(t) is the SOI and b(t) the RFI. In radio astronomy, u(t) is assumed to be a centred stationary "almost white" Gaussian noise. In our case, b(t) is a centred cyclostationary signal.

For the simulations, b(t) corresponds to a real RFI: Iridium. The Iridium system is a telecommunication satellites constellation using a combination of TDMA and FDMA techniques. In each channel, a QPSK modulation is performed. The synthesized signal has been simulated according to the Iridium emitted signal specifications [3].

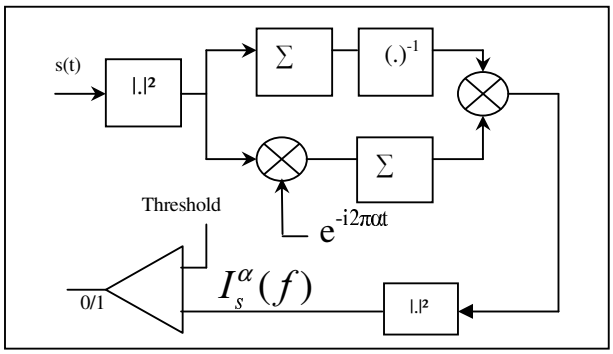

Figure 2: Functional description of the detector given by Equ. 2.

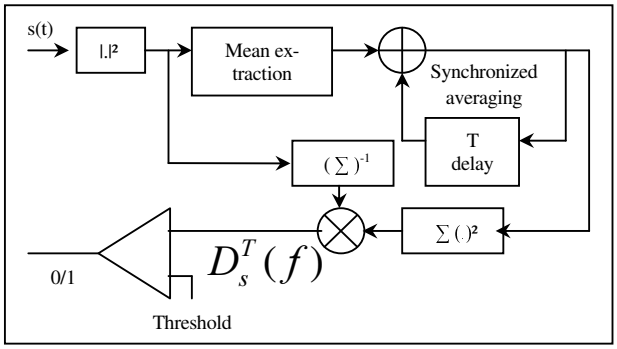

Figure 3: Functional description of the detector given by Equ. 3.

3. THE CYCLOSTATIONNARY DETECTORS

A signal s(t) is said to be cyclostationary if its autocorrelation function $R_s(t,\tau)$ is T-periodic in t [4]. The inverse of this period T is called the cyclic frequency α. The Fourier coefficients of $R_s(t,\tau)$ are $R_s^\alpha(\tau)$, called the cyclic autocorrelation functions:

$$R_s^\alpha(\tau) = E\left[s(t+\frac{\tau}{2}).s^*(t-\frac{\tau}{2}).e^{-i2\pi\alpha t} \right].$$

The frequency representation of $R_s^\alpha(\tau)$ is $S_s(\alpha, f)$, the cyclic spectrum. The interesting point is that, $S_s(\alpha, f)$ is non zero at $\{\alpha = k/T, k \in \mathbb{N}\}$, for cyclostationary signals. Besides, for non-cyclosationary signals, such as the SOI, the corresponding information is concentrated in α = 0. Thus, the presence of significant power at the discrete frequencies $\{\alpha = k/T, k \in \mathbb{N}^*\}$ is a discriminating indicator of a cyclostationary RFI.
The next subsections present two methods to detect such a signal. They are first described and then compared on several parameters.

3.1 Detectors description

The first detector is based on a method recently proposed by Raad et *al.* [5]. The principle is to integrate all the spectral information of a cyclostationary signal through the cyclic autocorrelation function at zero lag. The indicator is the following one:

$$I_s = \frac{\sum_{\alpha \neq 0} \left| R_s^\alpha(0) \right|^2}{\left| R_s^0(0) \right|^2}.$$

In our radio astronomical context, the cyclic frequency, α, is known and the received signal is channelized through the filter bank. Thus, the indicator can be expressed:

$$I_s^\alpha(f) = \frac{\left| R_s^\alpha(0) \right|^2}{\left| R_s^0(0) \right|^2} = \left| \frac{\sum_t \left| s(t,f) \right|^2 .e^{-i2\pi\alpha t}}{\sum_t \left| s(t,f) \right|^2} \right|^2, \quad (2)$$

where *f* is the channel number and *s(t,f)*, a sample of the time-frequency plane.
The algorithm of this detector is shown Fig. 2.

The second detector was introduced earlier by Weber et *al.* [6]. The principle is to detect spectral lines on the projection of the cyclic spectrum upon the α cyclic frequency axis. The complete algorithm reduces to a comb filtering of the square modulus of the analytical version of the signal. As previously, this detector can be adapted to our context. Thus, the criterion can be written as:

$$D_s^T(f) = \frac{\sum_t \left| H_T \otimes \left| s(t,f) \right|^2 \right|^2}{\sum_t \left| s(t,f) \right|^2}, \quad (3)$$

where H_T is a comb filter obtained by synchronized averaging over the periodicity T and ⊗ the convolution operator.
The algorithm of this detector is shown Fig. 3.

In fact, both methods are looking for periodicities on $\left| s(t,f) \right|^2$, a simple quadratic transformation of the signal. The difference is the kind of filter used to isolate the cyclic spectral lines. Consequently, their performances and their implementation may also differ.

3.2 Detector comparison

Two parameters are studied in the comparison of the detectors: N, the number of samples and the ISR. The first one is related to the blanking resolution; the smallest N is, the more accurate the blanking becomes. The second one is linked to the blanking sensitivity.
The Fisher criterion, C_F, is used to compare the two detectors:

$$C_F = \frac{\left(E_{H1}[C_D] - E_{H0}[C_D] \right)^2}{Var_{H1}[C_D] + Var_{H1}[C_D]},$$

where C_D is one of our two detectors $I_s^\alpha(f)$ or $D_s^T(f)$, E[.] the expectation and Var[.] the variance under the hypotheses H_0 and H_1 (see Equ. 1).

C_F represents the ratio of the distance between the hypotheses H_0 and H_1 in relation to their dispersion. The ideal detector would present a high Fisher criterion with low N and ISR. It is determined by Monte Carlo simulations. The results are shown on Fig. 4 with N varying from 128 to 4096 samples and ISR, from 5 to -10 dB. For each point of these curves, 100 runs have been performed. Besides, two kinds of cyclic frequencies have considered depending on whether $1/\alpha$ (i.e. T) is an integer or not.

Fig. 4a and 4c show the Fisher criterion computed for the first detector, $I_s^\alpha(f)$, and Fig. 4b for the second detector, $D_s^T(f)$. In Fig. 4a and 4b, $1/\alpha$ is 4 which is an integer unlike in Fig. 4c where $1/\alpha$ is 4.5.

The Fisher criterion grows up with N and ISR as expected. The methods presented here are both quite efficient when $1/\alpha$, is an integer, see Fig. 4a and 4b. $D_s^T(f)$ is even a little better than $I_s^\alpha(f)$ for high ISR. Nevertheless, their performances are quite equivalent when ISR is low. However it appears that $I_s^\alpha(f)$ is definitively better when $1/\alpha$ is not an integer (for the $\left[D_s^T(f), 1/\alpha = 4.5\right]$ case, the result were so poor (i.e. $C_F \leq 1$) that the curve has not been drawn).

Actually, the sampling frequency of the radio telescope is fixed, then $1/\alpha$ is rarely an integer unless the radio telescope receiver can be specifically reconfigured. This is generally difficult. Therefore, $I_s^\alpha(f)$ has been preferred for our RFI mitigation simulation.

4. EXAMPLE OF RFI MITIGATION

A time-frequency plane is synthesized to show the detector efficiency. An Iridium RFI is simulated. The resulting signal is shown in Fig. 5.a. It represents a signal of 6.4 MHz divided into 128 channels for a length of 90 ms. The Iridium signal occupies 6 different channels for several spaces of time. The ISR is –5 dB. It has been computed locally.

A sinusoidal signal has been added to simulate a non-cyclostationary RFI and a white Gaussian block noise is also present to simulate a strong SOI. The time integration of the time-frequency plane without blanking is presented in Fig. 5.b. The polluted channels and the sinusoidal signal, which are hard to detect in Fig. 5.a, are much more visible in Fig. 5.b. The strong added white Gaussian noise is quite visible in Fig. 5.a and Fig. 5.b.

The $I_s^\alpha(f)$ detector is applied on each channel of the signal with a sliding window of length N=512. The cyclic frequency to detect is α=0.25. The time integration of the signal after blanking is shown in Fig. 5.c. The RFI have been removed from the signal and the final spectrum is cleaned up. Only the sinusoidal signal and the strong white Gaussian noise are still visible.

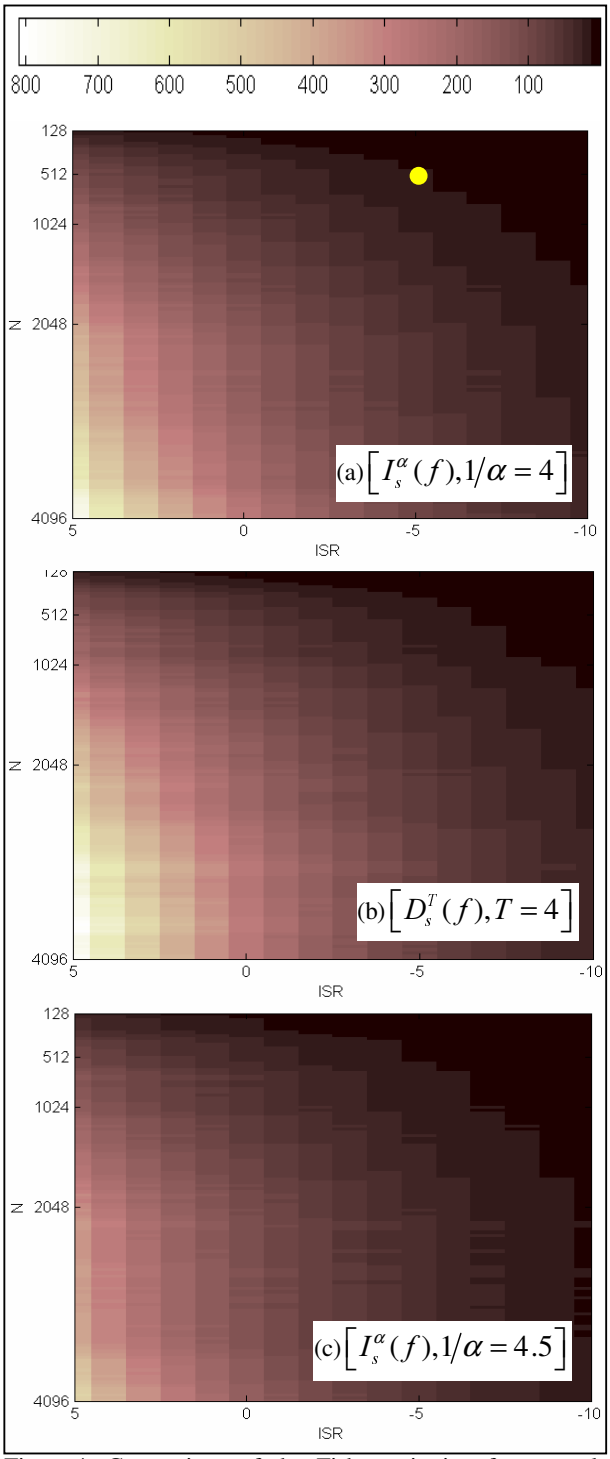

Figure 4: Comparison of the Fisher criterion for several values of N and ISR. N is the number of samples used by the detectors and ISR is the interference to signal ratio in dB. The yellow point in (a) corresponds to the parameters used for the simulation in section 4.

The detector has well blanked all the polluted signals (i.e. no non-detection). We observe that, 3.3 % of the received signal, shown in Fig. 5.a has been removed by blanking, while the actual RFI occupation rate is 2.7 %. This implies a very low level of false alarm rate (0.6%), concerning low N and ISR. This example shows that the chosen method is efficient to discriminate cyclostationary signals from stationary signals and is also robust against the brutal power fluctuation of the SOI, which is a real advantage compared to power detectors.

5. CONCLUSION

This paper deals with RFI mitigation for low ISR in the radio astronomy context by using the properties of cyclostationary RFI. Two detectors are compared. They are based on the same signal conditioning, which is a square modulus of the time-frequency plane. This quantity is easy to obtain in real time from radio astronomical receiver. Then, the detectors perform different filtering to detect the presence of RFI characteristic spectral lines. Finally, the most robust method has been used to perform a realistic simulation of time-frequency blanking. The results are a total detection of the cyclostationary RFI and a very good immunity to any, even strong, power fluctuations of the SOI. This last result could be very interesting in the case of bright and non-stationary SOI as solar or jovian emissions. The method must be validated now with real data and implemented for real time RFI mitigation.

REFERENCES

[1] P. A. Fridman and W. A. Baan, "RFI Mitigation Methods in Radio Astronomy," Astronomy & Astrophysics, vol. 378, pp.327-344, Oct. 2001.

[2] V. Clerc, R. Weber and C. Rosolen, "High Performance Receiver for RFI Mitigation in Radio Astronomy: Application at Decameter Wavelengths," in *Proc. EUSIPCO 2002*, Toulouse, France, Sept. 2002, pp. III-411 – III-414.

[3] R. J. Finean, "Mobile Satellite Communications Proposals," BT Technol Journal, vol. 14, n°3, pp 744 – 80, July. 1996.

[4] W. A. Gardner, Statistical Spectral Analysis – A Non-probabilistic Theory. New Jersey: Prentice Hall, 1988.

[5] A. Raad, J. Antoni and M. Sidahmed, "Indicators of Cyclostationary: Proposal, Statistical Evaluation and Application to Diagnostics," *in Proc. ICASSP 2003*, Hong Kong, April 2003, pp VI-757–VI-760.

[6] R. Weber and C. Faye, "Real Time Detector for Cyclostationary RFI in Radio Astronomy," in *Proc EUSIPCO* 1998, Island of Rhodes, Greece, Sept. 1998, pp. 1865-1868.

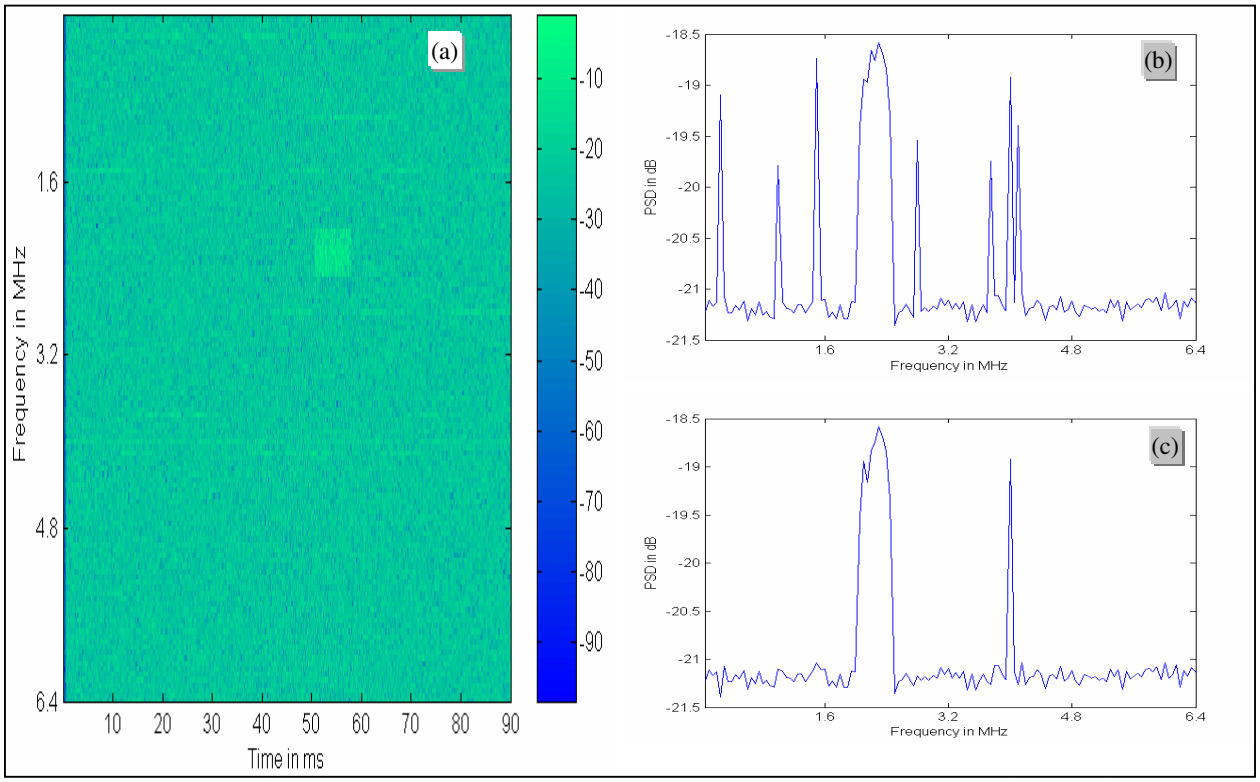

Figure 5: RFI mitigation of simulated Iridium RFI. (a) time-frequency representation of the polluted signal. Iridium bursts are present at 0.25 MHz, 1 MHz, 1.5 MHz, 2.8 MHz, 3.75 MHz and 4.1 MHz. The ISR is -5 dB. A sine wave is added at 4 MHz. A strong SOI is visible around 55 ms and 2.2 MHz. (b) Time integration without blanking. (c) Time integration with time blanking. All Iridium bursts have been removed. The integrity of the SOI is preserved.